

Digital Twin-Based User-Centric Edge Continual Learning in Integrated Sensing and Communication

Shisheng Hu*, Jie Gao[†], Xinyu Huang*, Mushu Li[‡], Kaige Qu*, Conghao Zhou*, and Xuemin (Sherman) Shen*

* Department of Electrical and Computer Engineering, University of Waterloo, Canada

[†]School of Information Technology, Carleton University, Canada

[‡] Department of Electrical, Computer, and Biomedical Engineering, Toronto Metropolitan University, Canada

Email: {s97hu, x357huan, k2qu, c89zhou, sshen}@uwaterloo.ca, jie.gao6@carleton.ca, mushu1.li@ryerson.ca

Abstract—In this paper, we propose a digital twin (DT)-based user-centric approach for processing sensing data in an integrated sensing and communication (ISAC) system with high accuracy and efficient resource utilization. The considered scenario involves an ISAC device with a lightweight deep neural network (DNN) and a mobile edge computing (MEC) server with a large DNN. After collecting sensing data, the ISAC device either processes the data locally or uploads them to the server for higher-accuracy data processing. To cope with data drifts, the server updates the lightweight DNN when necessary, referred to as continual learning. Our objective is to minimize the long-term average computation cost of the MEC server by optimizing two decisions, i.e., sensing data offloading and sensing data selection for the DNN update. A DT of the ISAC device is constructed to predict the impact of potential decisions on the long-term computation cost of the server, based on which the decisions are made with closed-form formulas. Experiments on executing DNN-based human motion recognition tasks are conducted to demonstrate the outstanding performance of the proposed DT-based approach in computation cost minimization.

Index Terms—Digital twin, integrated sensing and communication (ISAC), edge intelligence.

I. INTRODUCTION

Integrated sensing and communication (ISAC), emerging as a promising element of the sixth generation (6G) networks, has the potential to offer ubiquitous sensing services by utilizing wireless infrastructures [1], [2]. With artificial intelligence (AI) techniques, in particular deep neural networks (DNNs), sensing data collected in an ISAC system can be processed to detect human presence and comprehend the surrounding environments. This enhances user experience in applications such as smart homes and smart factories [3]. To process the potentially massive sensing data, the distributed computing resources within a wireless network can be utilized. First, some of the sensing data can be offloaded to a mobile edge computing (MEC) server for processing by a large and highly accurate pre-trained DNN [3]. Second, a *specialized* lightweight DNN [4] can be deployed on an ISAC device (e.g., an user equipment with both communication and radar modules [5]), which is trained to process sensing data of a relatively stationary distribution.

However, the sensing data collected by an ISAC device can follow a time-varying distribution. For example, when employing a time-division scheme in an ISAC system, the

duration allocated for sensing can be altered based on the communication demands of users, which leads to the change of the time dimension in the spectrogram of the sensing data. If the distribution of the currently collected sensing data diverges from that of the data used for training the lightweight DNN, a *data drift* occurs, which can degrade the accuracy of the lightweight DNN on the ISAC device. In this case, the lightweight DNN on the ISAC device needs to be updated. The update can be achieved by either delivering a suitable lightweight DNN from the server if available [6] or having the server retrain the lightweight DNN based on the sensing data after the data drift [7]. The latter method is referred to as edge continual learning.

Existing works on edge continual learning mainly focus on determining the selection (e.g., [4]) and the scheduling (e.g., [8]) of the training samples for balancing the training cost and the enhanced accuracy of the retrained DNN. When the server is involved in both sensing data processing and lightweight DNN retraining, two challenges arise. First, since each sample selected by the server for retraining the lightweight DNN is offloaded from the ISAC device, the decisions on the sensing data offloading and training data selection are inherently coupled. Second, the accuracy of a retrained lightweight DNN is insufficient to characterize the gain of the DNN retraining since the retrained lightweight DNN will be replaced after the next data drift occurs. Moreover, it is difficult to evaluate the gain beforehand due to the dynamic and user-specific nature of both the accuracy (as a function of training data selection) and the data drift.

In this paper, based on the digital twin (DT) paradigm [9]–[11], we propose a novel user-centric approach in an ISAC system. Our objective is to minimize the long-term average computation cost of an MEC server for sensing data processing and DNN retraining by jointly optimizing the decisions on sensing data offloading and training data selection. The main contributions of this paper are summarized as follows:

- We develop a DT-based approach to user-centric edge continual learning, which can capture the user’s unique time-varying communication demands and predict the gain of edge continual learning for the corresponding ISAC device.
- We design an efficient algorithm for sensing data

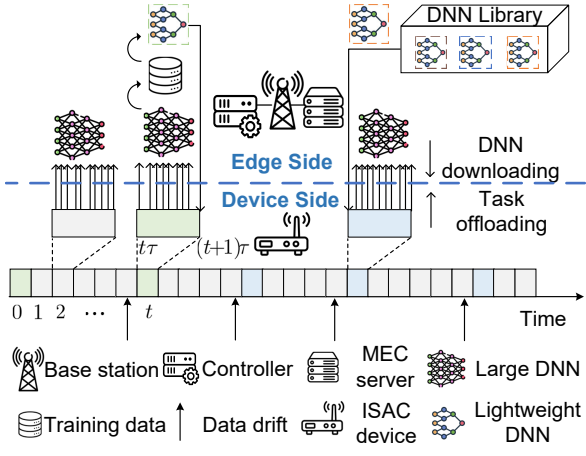


Fig. 1: System model.

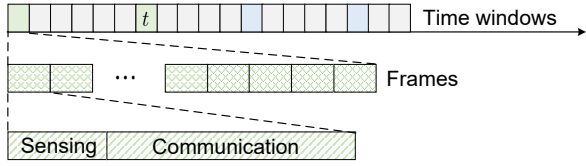


Fig. 2: Illustration of time windows and frames.

offloading and training data selection in edge continual learning based on the prediction results from the DT. Experiments on executing human motion recognition tasks are conducted to show that with the designed algorithm, the long-term average computation cost of the server can be largely reduced.

II. SYSTEM MODEL AND PROBLEM FORMULATION

A. Network Model

As shown in Fig. 1, we consider a scenario where an ISAC device, e.g., a user equipment with both communication and sensing modules, is deployed in an area for sensing and communication. An MEC server is deployed co-located with a base station to assist the device in processing the sensing data. As shown in Fig. 2, time is divided into time windows, each with a length of τ seconds, and the index of a time window is denoted by $t \in \{1, 2, 3, \dots\}$. Each time window consists of N frames of the same length. Similar to [12], the time-division scheme is adopted by the ISAC device. Specifically, in each frame, the device first transmits a sensing signal and receives the echo signal from the target. In the remaining time of the frame, the device transmits communication signals.

B. Sensing Task Generation and Processing

In each frame, the ISAC device preprocesses the received echo signal by extracting features from the echo signal, such as a time-Doppler spectrogram [12], to create a sensing data sample in this frame. A sensing task is then generated by the ISAC device to process the sensing data sample by a DNN (e.g., human motion recognition and fall detection). Each sensing task can be either *i*) offloaded to the MEC server to be processed by a large pre-trained DNN, or *ii*) locally

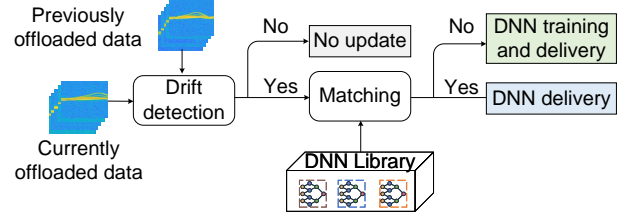


Fig. 3: The procedure to determine whether and how to update the lightweight DNN at the ISAC device.

processed by a lightweight DNN. We consider a probabilistic task offloading policy. Specifically, in the t -th time window, a sensing task generated in each frame is offloaded to the server with an *offloading probability* of $\rho_t \in [0, 1]$ and is locally processed with a probability of $1 - \rho_t$. The average accuracy of the sensing tasks in the t -th time window, denoted by A_t , is calculated as:

$$A_t = (1 - \rho_t)A_t^D + \rho_t A^E, \quad (1)$$

where $A_t^D \in [0, 1]$ represents the average accuracy of the on-device lightweight DNN over sensing data samples in the t -th time window, and A^E represents the average accuracy of the large DNN on the server. The large DNN with massive parameters is offline trained by a large dataset of the labeled sensing data samples, and we assume that the large pre-trained DNN on the server is perfectly accurate, i.e., $A^E = 1$.

Let O_t^I represent the expected computation cost of the server for processing the sensing tasks offloaded from the device in the t -th time window. It can be calculated as $O_t^I = N\rho_t c^I$, where c^I represents the average computation cost in terms of the number of floating-point operations (FLOPs) to process each sensing task by the large DNN at the server.

C. Updating the Lightweight DNN on the ISAC Device

For an ISAC device, a data drift can occur due to the time-varying resource availability for sensing. For example, in smart home applications, the average available sensing time can change depending on whether the user is conducting activities with high communication demands such as video streaming. The user's communication activities affect the device's sensing duration, which in turn may alter the distribution of the time-Doppler spectrogram of the sensing data. Without loss of generality, we assume that a data drift can occur at most once in any given time window. If a data drift occurs, the distribution of the sensing data changes and then remains the same until the next data drift. As shown in Fig. 3, at the beginning of each time window, a drift detection algorithm (e.g., [7]) is applied to determine whether a data drift occurs in the previous time window. If a data drift is detected, denoted by $I_t = 1$, the lightweight DNN at the ISAC device needs to be updated in either of the following two cases. Otherwise, we have $I_t = 0$.

1) *When a matched DNN is absent:* The server hosts a DNN library, containing several pre-trained lightweight DNNs. Each lightweight DNN is trained using sensing data from a distinct data distribution. If no lightweight DNN in the

DNN library is a match for the data distribution after a data drift, denoted by $M_t = 0$ (represented by the green blocks in Fig. 1 and Fig. 3), the server will retrain the lightweight DNN for the ISAC device. In the first $\tau - \mu$ seconds of the t -th time window, after a sensing task is offloaded to and processed by the server using a large DNN, the sensing data and sensing result are selected to construct one training sample for retraining the lightweight DNN with a *training probability* of $\gamma_t \in (0, 1]$. As a result, the expected number of samples used to retrain the lightweight DNN in the t -th time window is $\eta N \rho_t \gamma_t$, where $\eta = (\tau - \mu)/\tau$. In the final μ seconds of this time window, the server will retrain the lightweight DNN and deliver the retrained DNN to the ISAC device.

2) *When a matched DNN exists*: If a lightweight DNN in the DNN library is a match for the data distribution after the data drift, which we denote by $M_t = 1$ (represented by the blue blocks in Fig. 1 and Fig. 3), the server will deliver the DNN (with its accuracy known) to the ISAC device by the beginning of the next time window [6]. In this case, we have $\gamma_t = 0$.

An updated DNN will be used for the on-device processing of sensing tasks until the next data drift is detected. The expected computation cost of retraining the lightweight DNN in the t -th time window is denoted by O_t^R and can be calculated as $O_t^R = \eta N \rho_t \gamma_t c^R$, where c^R represents the average computation cost, in terms of the number of FLOPs, for using each training sample to retrain the lightweight DNN.

D. Problem Formulation

The expected accuracy of the sensing tasks in each time window should be higher than a threshold:

$$A_t \geq A^{\min}, \quad \forall t \in \{1, 2, 3, \dots\}, \quad (2)$$

where $A^{\min} \in [A_t^D, 1]$. By combining (1) and (2), we can obtain the minimum task offloading probability in the t -th time window, denoted by ρ_t^{\min} , that satisfies the average accuracy requirement:

$$\rho_t^{\min} = 1 - \frac{1 - A^{\min}}{1 - A_t^D}. \quad (3)$$

In the beginning of each time window, a network controller determines the task offloading probability, ρ_t , and the training probability, γ_t , for the ISAC device in this time window. To support more ISAC devices, our objective is to minimize the average edge computation cost for the ISAC device over all time windows. The problem is formulated as:

$$(P1) \quad \min_{\{\rho_t, \gamma_t, t=1, 2, \dots, T\}} \lim_{T \rightarrow \infty} \frac{1}{T} \sum_{t=1}^T (N \rho_t c^I + \eta N \rho_t \gamma_t c^R), \quad (4a)$$

$$\text{s.t.} \quad \rho_t^{\min} \leq \rho_t \leq 1, \quad (4b)$$

$$0 \leq \gamma_t \leq \max\{(1 - M_t)I_t, 1\}, \quad (4c)$$

where (4b) ensures that the minimum task offloading probability in (3) should be attained to satisfy the accuracy requirement in (2). Constraint (4c) ensures that the lightweight

DNN is retrained by the server in a time window only if *i*) a data drift is detected in this time window, i.e., $I_t = 1$, and *ii*) there is no lightweight DNN in the DNN library that is a match for the current data distribution, i.e., $M_t = 0$.

In the time windows when the server does not need to retrain the lightweight DNN for the ISAC device, the optimal task offloading probability equals the minimum task offloading probability calculated in (3). To this end, in the following sections, unless specified otherwise, we consider the time windows in which $I_t = 1$ and $M_t = 0$.

III. DIGITAL TWIN-BASED USER-CENTRIC APPROACH FOR EDGE CONTINUAL LEARNING

It is difficult to solve (P1) directly since two pieces of important information needed for this problem are unknown in advance: *i*) whether a data drift will occur in a time window or not, for all the considered time windows, and *ii*) the accuracy of the lightweight DNN given a task offloading and training probability. To estimate the above information for accurately evaluating the decisions on the task offloading and training probabilities, we construct a DT of the ISAC device and propose a user-centric approach using the DT.

A. DT-Based Prediction of Data Drift Occurrence

The moment when the next data drift occurs is important for solving (P1) as it determines the number of time windows for which retraining the lightweight DNN can be beneficial. Let T_t represent the number of time windows up to the next data drift, and we have:

$$I_k = \begin{cases} 0, & \text{if } t+1 \leq k \leq t+T_t-1 \text{ and } T_t > 1, \\ 1, & \text{if } k = t+T_t. \end{cases} \quad (5)$$

Suppose that at the beginning of the t -th time window, $\sum_{k=1}^t I_k$ occurrences of data drift have been observed. Accordingly, $\sum_{k=1}^t I_k - 1$ time intervals between two consecutive data drifts can be obtained as a sequence $\mathcal{D}_t = \{D_1, D_2, \dots\}$, where D_i represents the number of time windows between the i -th data drift and the $(i+1)$ -th data drift, and $|\mathcal{D}_t| = \sum_{k=1}^t I_k - 1$. The average of the latest W values in \mathcal{D}_t is used as the DT model of the expected value of T_t , denoted by \bar{T}_t . At the beginning of the t -th time window, \bar{T}_t is updated as:

$$\bar{T}_t = \frac{\sum_{i=\max\{1, |\mathcal{D}_t| - W + 1\}}^{|\mathcal{D}_t|} D_i}{\max\{|\mathcal{D}_t|, W\}}. \quad (6)$$

B. DT-Based Prediction of Lightweight DNN Accuracy

The accuracy of the retrained lightweight DNN is also important for solving (P1) since it determines the minimum task offloading probability in (3) for the next T_t windows. The accuracy is generally non-decreasing with the number of training samples used to train the DNN, which is determined by ρ_t and γ_t in our considered problem. Such a relation can be time-varying based on the characteristic of the sensing data. For example, in Fig. 4, it is shown that with the sensing duration following two different uniform distributions, the

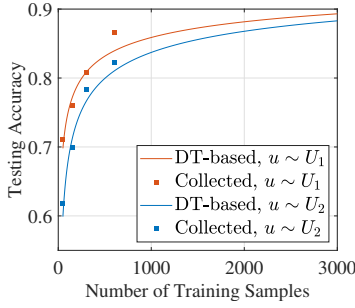


Fig. 4: The testing accuracy of human motion recognition by a lightweight DNN versus the number of training samples used, where u represents the sensing duration in a frame. See Section V for more details on the settings.

corresponding accuracy of a lightweight DNN retrained by using the same number of training samples can be different.

1) *DT Model*: Similar to [13], an exponential function is used to predict the accuracy of the retrained lightweight DNN:

$$A_k^D(x) = 1 - a_t x^{-b_t}, t + 1 \leq k \leq t + T_t, \quad (7)$$

where $A_k^D(x)$ represents the accuracy of the lightweight DNN that is trained by x samples in the t -th time window, and a_t and b_t are positive learnable parameters.

2) *DT Data Collection and DT Model Update*: From the training process in the t -th time window, K_t samples are collected:

$$\mathcal{N}_t = \{(x_1, A_{t,1}), (x_2, A_{t,2}), \dots, (x_{K_t}, A_{t,K_t})\}, \quad (8)$$

where $A_{t,i}$ represents the accuracy of the retrained lightweight DNN with x_i training samples in the t -th time window (e.g., $K_t = 4, x_1 = 50, x_2 = 150, x_3 = 300$, and $x_4 = 600$ in Fig. 4).

The parameters in the DT model are updated at the beginning of the $(t + 1)$ -th time window, by minimizing the mean square error of the accuracy prediction on the samples \mathcal{N}_t :

$$(a_{t+1}, b_{t+1}) = \arg \min_{a_{t+1}, b_{t+1}} \sum_{i=1}^{|\mathcal{N}_t|} \left(1 - a_{t+1} x_i^{-b_{t+1}} - A_{t,i}\right)^2. \quad (9)$$

3) *DT-Based DNN Accuracy Prediction*: Leveraging the DT, the accuracy of the retrained lightweight DNN in the k -th time window, i.e., $A_k^D(\rho_t, \gamma_t)$, given the task offloading and training decisions in the t -th time window, i.e., ρ_t and γ_t , can be predicted as:

$$A_k^D = 1 - a_t (\eta N \rho_t \gamma_t)^{-b_t}, t + 1 \leq k \leq t + T_t. \quad (10)$$

Then, the minimum task offloading probability in the k -th time window, where $t + 1 \leq k \leq t + T_t$, given by (3), can be calculated as:

$$\begin{aligned} \bar{\rho}_k^{\min}(\rho_t, \gamma_t) &= 1 - \frac{1 - A^{\min}}{a_t (\eta N \rho_t \gamma_t)^{-b_t}} \\ &\triangleq \bar{\rho}_{0,t}^{\min}(\rho_t, \gamma_t), t + 1 \leq k \leq t + T_t. \end{aligned} \quad (11)$$

C. DT-Based User-Centric Decision Evaluation

In the beginning of the t -th time window, with the prediction of the next data drift, we can estimate the expected number of time windows when the retrained lightweight DNN can be used, i.e., \bar{T}_t . With the DT-based prediction of the lightweight DNN's accuracy, we can estimate the minimum task offloading probability when the retrained lightweight DNN is used, i.e., $\bar{\rho}_{0,t}^{\min}(\rho_t, \gamma_t)$ in (11). As a result, we can estimate the expected computation cost of task processing for the edge server until the next data drift as $N \rho_t c^I + \bar{T}_t N \bar{\rho}_{0,t}^{\min}(\rho_t, \gamma_t) c^I$. Since retraining the lightweight DNN at the device can reduce the volume of sensing data to offload and in turn the associated edge computation cost, the decrease of this cost is the gain of DNN retraining. Adding this expected cost of task processing to the cost of DNN retraining, i.e., $N \rho_t \gamma_t c^R$, we define the long-term computation cost resulting from decisions ρ_t and γ_t , denoted by $O_t(\rho_t, \gamma_t)$ and calculated as:

$$O_t(\rho_t, \gamma_t) = N \rho_t \gamma_t c^R + N \rho_t c^I + \bar{T}_t N \bar{\rho}_{0,t}^{\min}(\rho_t, \gamma_t) c^I. \quad (12)$$

IV. PROBLEM TRANSFORMATION AND SOLUTION

With the DT-based prediction results, we transform the long-term optimization problem into consecutive one-shot optimization problems. Specifically, in the beginning of a time window when the lightweight DNN needs to be retrained, the optimal task offloading and training probabilities in this time window should minimize the long-term computation cost:

$$(P2) \min_{\rho_t, \gamma_t} O_t(\rho_t, \gamma_t) \quad (13a)$$

$$\mathbf{s.t.} \quad \bar{\rho}_t^{\min} \leq \rho_t \leq 1, \quad (13b)$$

$$0 \leq \gamma_t \leq 1. \quad (13c)$$

A. Properties of the Transformed Problem

Proposition 1: If $0 < b_t < 1$, $O_t(\rho_t, \gamma_t)$ is a bi-convex function.

Proof. With γ_t fixed, the second partial derivative of O_t with respect to ρ_t is:

$$\frac{\partial^2 O_t}{\partial (\rho_t)^2} = \frac{1 - b_t}{a_t} \underbrace{\bar{T}_t \gamma_t^2 b_t (1 - A^{\min}) c^I \eta^2 N^3 (\eta N \rho_t \gamma_t)^{-2+b_t}}_{\geq 0}. \quad (14)$$

With ρ_t fixed, the second derivative of O_t with respect to γ_t is:

$$\frac{\partial^2 O_t}{\partial (\gamma_t)^2} = \frac{1 - b_t}{a_t} \underbrace{\bar{T}_t \rho_t^2 b_t (1 - A^{\min}) c^I \eta^2 N^3 (\eta N \rho_t \gamma_t)^{-2+b_t}}_{\geq 0}, \quad (15)$$

where the highlighted parts are positive since $A^{\min} \leq 1$.

As a result, if $0 < b_t < 1$, the two partial second derivatives are both positive. ■

Proposition 2: If $b_t \geq 1$, $O_t(\rho_t, \gamma_t)$ is a bi-concave function.

Proof. From (14) and (15), it can be observed that when $b_t \geq 1$, the second partial derivatives are both non-positive. ■

B. Algorithm

Based on the propositions, Algorithm 1 is proposed to efficiently solve (P2). Specifically, when $0 < b_t < 1$, since the objective function of is a bi-convex function and the constraints are convex, (P2) is a bi-convex optimization problem. In this case, an alternate convex search method [14] is used in Algorithm 1. When $b_t \geq 1$, the objective function of (P2) is a bi-concave function. In this case, the minimizer of the function can be obtained at the Cartesian product of the vertex sets of (13b) and (13c) [14, Theorem 3.10].

C. Closed-Form Solutions

If $0 < b_t < 1$, the closed-form solutions in each iteration of Algorithm 1 can be obtained. The partial derivatives of $O_t(\rho_t, \gamma_t)$ with respect to ρ_t and γ_t can be calculated by:

$$\frac{\partial O_t}{\partial \rho_t} = N c^I + N \gamma_t c^R - T_t \frac{(1 - A^{\min}) b_t c^I \eta N^2 \gamma_t (\eta N \rho_t \gamma_t)^{-1+b_t}}{a_t}, \quad (16)$$

$$\frac{\partial O_t}{\partial \gamma_t} = N c^R \rho_t - T_t \frac{(1 - A^{\min}) b_t c^I \eta N^2 \rho_t (\eta N \rho_t \gamma_t)^{-1+b_t}}{a_t}. \quad (17)$$

Given the offloading probability ρ_t , the training probability γ_t^o at which $\frac{\partial O_t}{\partial \gamma_t} |_{\gamma_t=\gamma_t^o} = 0$ can be calculated as:

$$\gamma_t^o = N^{\frac{b_t}{1-b_t}} \rho_t^{-1} \left(\frac{a_t c^R}{c^I \bar{T}_t \eta (1 - A^{\min}) b_t} \right)^{-\frac{1}{1-b_t}}. \quad (18)$$

Given the training probability γ_t , the offloading probability ρ_t^o at which $\frac{\partial O_t}{\partial \rho_t} |_{\rho_t=\rho_t^o} = 0$ can be calculated as:

$$\rho_t^o = N^{\frac{b_t}{1-b_t}} (\eta \gamma_t)^{-1} \left(\frac{a_t (1 + \gamma_t c^R)}{c^I \bar{T}_t \eta (1 - A^{\min}) b_t \gamma_t} \right)^{-\frac{1}{1-b_t}}. \quad (19)$$

Proposition 3: The optimal training probability that minimizes the long-term computation cost, denoted by γ_t^{opt} , when the offloading probability is ρ_t , can be calculated as:

$$\gamma_t^{\text{opt}} = \begin{cases} \gamma_t^o, & \text{if } 0 \leq \gamma_t^o \leq 1, \\ 1, & \text{otherwise.} \end{cases} \quad (20)$$

The optimal task offloading probability that minimizes the long-term computation cost, denoted by ρ_t^{opt} , when the training probability is γ_t , can be calculated as:

$$\rho_t^{\text{opt}} = \begin{cases} \rho_t^{\min}, & \text{if } \rho_t^o \leq \rho_t^{\min}, \\ \rho_t^o, & \text{if } \rho_t^{\min} \leq \rho_t^o \leq 1, \\ 1, & \text{otherwise.} \end{cases} \quad (21)$$

Proof. Omitted here due to space limitation. ■

Remark 1: Since $\frac{1}{-1+b_t}$ in (18) is negative, the optimal training probability in (20) increases with the expected number of time windows up to the next data drift, i.e., \bar{T}_t . This is expected since in this case a retrained lightweight DNN can be used for more time windows on average, and it is thus advantageous to increase the accuracy of the lightweight DNN by constructing and using more training samples.

Algorithm 1 Joint Optimization of Sensing Task Offloading and Selection for Edge Continual Learning

```

1: if  $0 < b_t < 1$  then
2:    $i \leftarrow 0$ 
3:   Initialize  $\rho_t^{(0)}$  by randomly choosing from  $[\rho_t^{\min}, 1]$ .
4:   repeat
5:      $i \leftarrow (i + 1)$ 
6:     Given  $\rho_t^{i-1}$ , find optimal  $\gamma_t^i \in [0, 1]$  that minimizes
        $O_t(\rho_t^{i-1}, \gamma_t^i)$  based on (18) and (20).
7:     Given  $\gamma_t^i$ , find optimal  $\rho_t^i \in [\rho_t^{\min}, 1]$  that minimizes
        $O_t(\rho_t^i, \gamma_t^i)$  based on (19) and (21).
8:     until  $|\rho_t^{(i)} - \rho_t^{(i-1)}|$  and  $|\gamma_t^{(i)} - \gamma_t^{(i-1)}| < 10^{-2}$ 
9:      $\rho_t^* \leftarrow \rho_t^i, \gamma_t^* \leftarrow \gamma_t^i$ 
10:  end if
11: if  $b_t \geq 1$  then
12:    $(\rho_t^*, \gamma_t^*) = \arg \min_{\rho_t \in \{\rho_t^{\min}, 1\}, \gamma_t \in \{0, 1\}} O_t(\rho_t, \gamma_t)$ 
13: end if
Output:  $\rho_t^*, \gamma_t^*$ 

```

V. SIMULATION RESULTS

In this section, we evaluate the performance of the proposed DT-based edge continual learning for a radar sensing-based human motion recognition task in [12], which classifies human motion into *standing*, *child pacing*, *child walking*, *adult pacing*, and *adult walking*. The settings of the radar sensing parameters, including the bandwidth, carrier frequency, sweep time of a frequency-modulated continuous wave (FMCW) sensing signal, and the height and speed of the sensing target are set following [12]. The signal reflected from a sensing target is simulated using the Phased Array System Toolbox of MATLAB. The received signal undergoes the following preprocessing steps, *i*) sampling (at the frequency given by [12]), *ii*) mix with a reference signal, *iii*) short-time Fourier transform (STFT), and *iv*) normalization and conversion into a 256×256 spectrogram. Each lightweight DNN consists of one convolutional layer and two fully-connected layers, and the computation cost for training it using each sample, i.e., c^R , is 24.9 GFLOPs [15]. ResNet-18 is selected as the large DNN, and the computation cost of using it for processing each task, i.e., c^I , is 4.5 GFLOPs.

The occurrence of a data drift in the t -th time window follows a Bernoulli distribution with the parameter P_t^{dr} . We consider in total $T = 1 \times 10^5$ time windows with $P_t^{\text{dr}} = P_0^{\text{dr}}, \forall t = 1, 2, 3, \dots, T/2$, and $P_t^{\text{dr}} = P_0^{\text{dr}}/4, \forall t = T/2 + 1, \dots, T$. In each time window, there are $N = 1500$ frames and $\eta = 0.8$. In addition, M_t follows a Bernoulli distribution with the parameter $P^{\text{md}} = 0.75$. Moreover, the relation between the accuracy of a retrained lightweight DNN and the number of the training samples varies over time following a two-state Markov process. The transition matrix of the Markov process is $[\sigma, 1 - \sigma; 1 - \sigma, \sigma]$, where $\sigma = 0.3$ represents the probability that the relation remains unchanged when the lightweight DNN needs to be retrained. A state of the relation is described by the parameters (a_t, b_t) in the DT model for predicting the accuracy in (10). As shown in Fig. 4, two sets of the parameters are obtained when the sensing time in each frame follows $U(0.6, 0.8)$ and $U(0.4, 0.8)$ seconds, and the values are (0.81, 0.25) and (1.30, 0.30) based on (9).

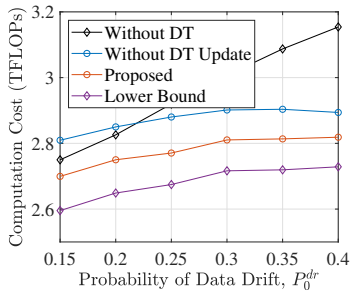


Fig. 5: Average computation cost of the server versus the probability of data drift P_0^{dr} .

We consider the following three benchmarks.

- **Lower Bound:** The occurrence of a data drift in all the time windows and the relation between the accuracy of a retrained lightweight DNN and the number of training samples are perfectly known a priori.
- **Without DT Update:** The parameters for DNN accuracy prediction and the expected time interval between two consecutive data drifts are first estimated and then assumed unchanged.
- **Without DT:** When the lightweight DNN needs to be retrained, the minimum task offloading probability is selected, i.e., $\rho_t = \rho_t^{\min}$, and all the offloaded sensing tasks are used for retraining, i.e., $\gamma_t = 1$.

In Fig. 5, the average edge computation cost per time window versus the probability of the data drift, i.e., P_0^{dr} , is shown. It can be observed that the proposed DT-based approach outperforms both the approach without DT and that without DT update. In addition, the performance gain over the approach without DT increases with the probability of data drift occurrence. This is expected as the proposed approach uses the DT to estimate the time duration when a retrained lightweight DNN can be used in determining the training probability, while the approach without the DT uses all the offloaded sensing tasks and their results to retrain the lightweight DNN. In Fig. 6, given $P_0^{dr} = 0.3$, the training probability versus the index of the time window is shown. It can be observed that by the proposed approach, in the second half of the time windows, the training probability is increased. This is expected as the probability of a data drift is set to decrease after the $(T/2 + 1)$ -th time window, and the expected time interval between two consecutive data drifts thus increases. Based on Remark 1, the optimal training probability should increase in this case. By comparison, without updating the DT to capture such a change, the training probability is not appropriately adjusted.

VI. CONCLUSION

We have proposed a DT-based approach for user-centric edge continual learning in an ISAC system. A DT of an ISAC device has been constructed to capture the corresponding user's unique time-varying communication demands and their impact on the gain of edge continual learning. Then, sensing data offloading and training data selection have been optimized for the user, subject to the user's task processing accuracy requirement, while minimizing the computation cost for the

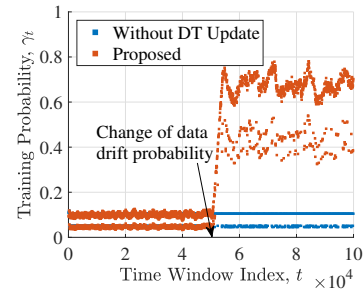


Fig. 6: Training probability versus time window index.

MEC server. The proposed approach to user-centric edge continual learning is a step toward seamless integration of sensing, communication, and computation in 6G networks. For future work, we will investigate DT-based joint sensing, communication, and computing resource reservation for edge continual learning in a multi-device scenario.

REFERENCES

- [1] F. Liu, Y. Cui, C. Masouros, J. Xu, T. X. Han, Y. C. Eldar, and S. Buzzi, "Integrated sensing and communications: Toward dual-functional wireless networks for 6G and beyond," *IEEE J. Sel. Areas Commun.*, vol. 40, no. 6, pp. 1728–1767, 2022.
- [2] J. Chen, X. Wang, and Y.-C. Liang, "Impact of channel aging on dual-function radar-communication systems: Performance analysis and resource allocation," *IEEE Trans. Commun.*, vol. 71, no. 8, pp. 4972–4987, 2023.
- [3] W. Xu, Z. Yang, D. W. K. Ng, M. Levorato, Y. C. Eldar, and M. Debbah, "Edge learning for B5G networks with distributed signal processing: Semantic communication, edge computing, and wireless sensing," *IEEE J. Sel. Topics Signal Process.*, vol. 17, no. 1, pp. 9–39, 2023.
- [4] Y. Yang, M. Sankaradas, and S. Chakradhar, "Dyco: Dynamic, contextualized AI models," *ACM Trans. Embed. Comput. Syst.*, vol. 21, no. 6, pp. 1–21, Dec. 2022.
- [5] K. Ji, Q. Zhang, Z. Wei, Z. Feng, and P. Zhang, "Networking based ISAC hardware testbed and performance evaluation," *IEEE Commun. Mag.*, vol. 61, no. 5, pp. 76–82, 2023.
- [6] K. Huang, H. Wu, Z. Liu, and X. Qi, "In-situ model downloading to realize versatile edge AI in 6G mobile networks," *IEEE Wireless Commun.*, vol. 30, no. 3, pp. 96–102, 2023.
- [7] L. Wang, Z. Yu, H. Yu, S. Liu, Y. Xie, B. Guo, and Y. Liu, "Adaevco: Edge-assisted continuous and timely DNN model evolution for mobile devices," *IEEE Trans. Mobile Comput.*, pp. 1–18, 2023, to be published.
- [8] L. Jia, Z. Zhou, F. Xu, and H. Jin, "Cost-efficient continuous edge learning for artificial intelligence of things," *IEEE Internet of Things J.*, vol. 9, no. 10, pp. 7325–7337, 2022.
- [9] X. Shen, J. Gao, W. Wu, M. Li, C. Zhou, and W. Zhuang, "Holistic network virtualization and pervasive network intelligence for 6G," *IEEE Commun. Surveys Tuts.*, vol. 24, no. 1, pp. 1–30, 2022.
- [10] S. Hu, M. Li, J. Gao, C. Zhou, and X. Shen, "Digital twin-assisted adaptive DNN inference in industrial Internet of Things," in *Proc. IEEE Global Commun. Conf. (GLOBECOM)*, 2022, pp. 1025–1030.
- [11] C. Zhou, J. Gao, M. Li, X. Shen, and W. Zhuang, "Digital twin-empowered network planning for multi-tier computing," *J. Commun. Inf. Netw.*, vol. 7, no. 3, pp. 221–238, 2022.
- [12] P. Liu, G. Zhu, S. Wang, W. Jiang, W. Luo, H. V. Poor, and S. Cui, "Toward ambient intelligence: Federated edge learning with task-oriented sensing, computation, and communication integration," *IEEE J. Sel. Topics Signal Process.*, vol. 17, no. 1, pp. 158–172, 2023.
- [13] S. Wang, Y.-C. Wu, M. Xia, R. Wang, and H. V. Poor, "Machine intelligence at the edge with learning centric power allocation," *IEEE Trans. Wireless Commun.*, vol. 19, no. 11, pp. 7293–7308, 2020.
- [14] J. Gorski, F. Pfoeffler, and K. Klamroth, "Biconvex sets and optimization with biconvex functions: a survey and extensions," *Math. Methods Oper. Res.*, vol. 66, pp. 373–407, 2007.
- [15] J. Sevilla, L. Heim, M. Hobbhahn, T. Besiroglu, A. Ho, and P. Villalobos, "Estimating training compute of deep learning models," 2022. [Online]. Available: <https://epochai.org/blog/estimating-training-compute>